

Low-Speed Gas Flow Subchoking Phenomenon in a Long-Constant-Area Microchannel

Zhao-hui Yao,* Feng He,* Ying-tao Ding,† Meng-yu Shen,‡ and Xue-fang Wang‡
Tsinghua University, 100084 Beijing, People's Republic of China

The study on gas flow characteristics in a long-constant-area microchannel in mixed Knudsen-number-regime flows has not only theoretical meaning, but also important application in controlling outer-space aerocrafts. Flow characteristics were studied based on the experiment and approximate theoretical analysis. The inlet pressure was 130, 250, and 320 kPa, and the outlet pressure ranged from 9 to 100 kPa. Five pressure measuring points were distributed along the microchannel, and the temperature sensors were located at the inlet and outlet. The pressure distribution and the volume flow rate of air were measured experimentally. An approximate theoretical model based on Poiseuille flow was applied. Experimental investigations with the long-constant-area microchannel indicate that the mass flow rate through the microchannel changes little as the inlet-to-outlet pressure ratio reaches some critical pressure ratio. The phenomenon is defined as subchoking, and the corresponding pressure ratio is defined as the subchoking critical pressure ratio. The phenomenon of subchoking is caused by the surface effects. Moreover, the effects of the ratio of surface to volume on the critical pressure ratio are studied.

Nomenclature

H	=	microchannel height
Kn	=	Knudsen number
L	=	microchannel length
\dot{M}	=	mass flow rate
$(\dot{M})_{\max}$	=	maximum mass flow rate
Ma	=	Mach number
p	=	pressure
p_{in}	=	inlet pressure
$(p_{\text{in}}/p_{\text{out}})_{\text{sc}}$	=	subchoking critical pressure ratio
p_{out}	=	outlet pressure
R	=	gas constant
Re	=	Reynolds number
T	=	temperature
w	=	microchannel width
x	=	Cartesian body axes
μ	=	dynamic viscosity
Π_i	=	inlet-to-outlet pressure ratio
σ_v	=	tangential momentum accommodation coefficient

Subscripts

in	=	inlet
max	=	maximum
out	=	outlet
sc	=	subchoking

I. Introduction

CONSIDER a long-constant-area microchannel where the entrance pressure is atmospheric and the exit conditions are near vacuum. As air goes down the duct, the pressure and density decrease while the velocity, Mach number, and Knudsen number increase. With lower density, the mean free path increases, and the Knudsen number correspondingly increases. All flow regimes can

occur in the same microchannel: continuum with no-slip boundary conditions, slip-flow regime, transition regime, and free-molecule flow.

The study on gas flow characteristics in a long-constant-area microchannel in mixed Knudsen-number-regime flows has not only theoretical meaning, but also important application in controlling outer-space aerocrafts. Different researchers^{1–4} studied Knudsen-number-regime gas flow characteristics in different ways, such as experimental method, theoretical method, and so on. But there are rarely reports about multiregime mixed gas flow characteristics.

Most researchers measured experimentally the outlet volume flow rate for some specified inlet-to-outlet pressure ratio. As a result, the experimental information was limited. In 1994, with the use of microchannel distributed pressure sensors,⁴ the experimental information was more significant. But these experiments specified the outlet pressure as 1 atm, and the inlet-to-outlet pressure ratio was relatively low (lower than 4.0). Because of the low pressure ratio, it is difficult to realize flow with regions in different regimes including continuum flow, slip flow, and transition flow. The theoretical analysis was based on the approximate theoretical model,⁵ which was two-dimensional, partially considering compressibility. As the Knudsen number is lower than 0.1, the model is applicable.

Gas flow characteristics in single flow regime have been studied. In this paper, a rectangular cross-section long-constant-area microchannel with distributed pressure sensors was fabricated based on the microfabrication technology. The experimental results show that the mass flow rate through the microchannel changes little as the inlet-to-outlet pressure ratio reaches some critical pressure ratio.

II. Experimental Research and Result Analysis

The geometry schematic of the microchannel and the experimental apparatus are shown in Figs. 1 and 2. The rectangular cross-section microchannel is 39.9 mm long, 1000 μm wide, and 7 μm deep. Inlet total pressure and outlet pressure are given, while other parameters such as the outlet volume flow rate, inlet and outlet temperature, and pressure distribution are measured. The pressure distribution is calibrated based on Electronic Pressure Scanning Modules in Hyscan 2000. For isothermal flow, Knudsen number is inversely proportional to local pressure, so by regulating the pressure values, multiregime mixed-flow phenomenon can be realized. During the experiment, air is used as working medium, the outlet pressure is lower than 1 atm, and the inlet pressure is higher than 1 atm. The experimental error analysis is shown in Appendix A.

Keeping the inlet pressure constant and regulating the outlet pressure, the mass flow rate and pressure distribution for different

Received 4 August 2003; revision received 28 March 2004; accepted for publication 29 March 2004. Copyright © 2004 by the American Institute of Aeronautics and Astronautics, Inc. All rights reserved. Copies of this paper may be made for personal or internal use, on condition that the copier pay the \$10.00 per-copy fee to the Copyright Clearance Center, Inc., 222 Rosewood Drive, Danvers, MA 01923; include the code 0001-1452/04 \$10.00 in correspondence with the CCC.

*Associate Professor, Department of Engineering Mechanics.

†Postdoctoral Researcher, Department of Engineering Mechanics.

‡Professor, Department of Engineering Mechanics.

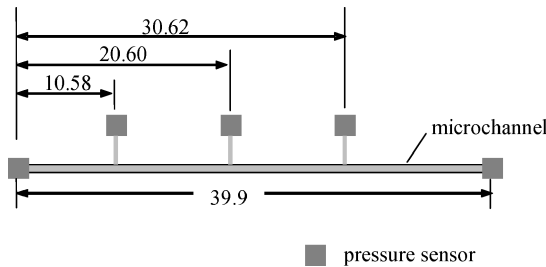


Fig. 1 Sketch of a long-constant-area microchannel (units in millimeters).

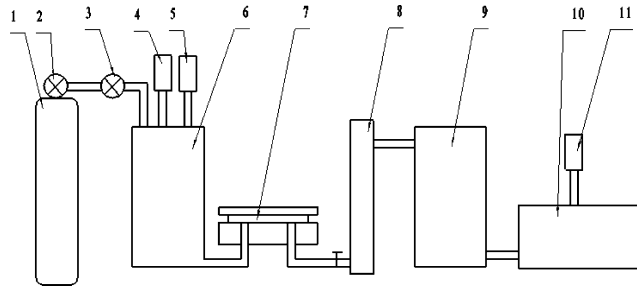


Fig. 2 Schematic of experimental apparatus: 1, high-pressure gas cylinder; 2, pressure regulator; 3, pressure regulator with fine filter; 4, pressure sensor; 5, temperature sensor; 6, stagnant chamber; 7, microchannel test section; 8, flow monitor apparatus; 9, stagnant chamber; 10, vacuum pump; and 11, vacuum pressure sensor.

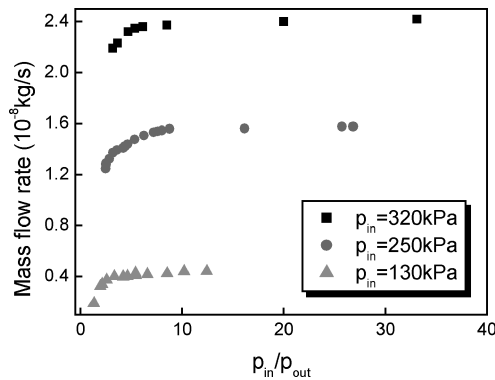


Fig. 3 Relationship curve between mass flow rate and inlet-to-outlet pressure ratio.

pressure ratios are obtained experimentally. Inlet pressure is 130, 250, and 320 kPa, outlet pressure ranges from 100 to 9 kPa. The experimental results are summarized in the tables seen in Appendix B. The relationship curve between mass flow rate and inlet-to-outlet pressure ratio is plotted in Fig. 3. The pressure distributions are shown in Fig. 4.

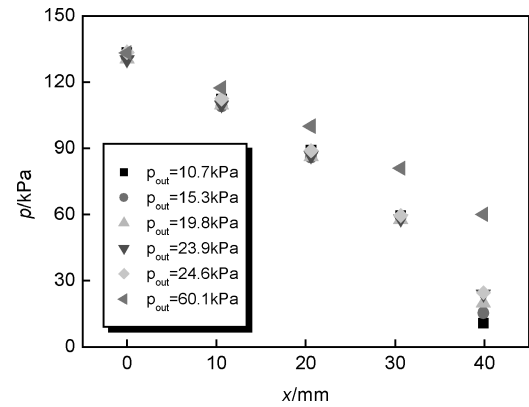
From Fig. 3, it can be seen that as the pressure ratio is lower than approximately 5.3 mass flow rate increases with the increase of pressure ratio; otherwise, as the pressure ratio is higher than 5.3 mass flow rate changes little with the increase of pressure ratio, tending to a constant.

From Fig. 4, it can be observed that pressure distribution is non-linear. When the pressure ratio is lower than approximately 5.3, pressure distribution changes greatly for different pressure ratios. But when the pressure ratio is higher than 5.3, pressure distribution changes little except near the outlet.

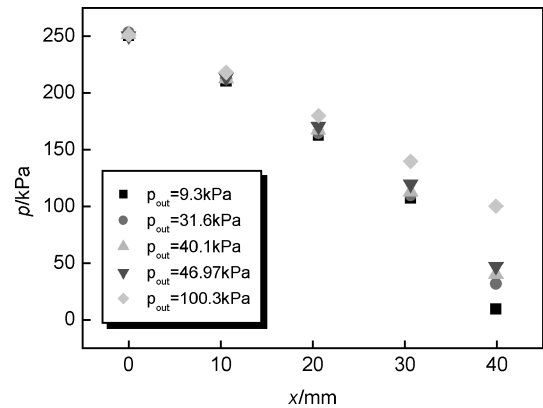
From the preceding analysis, it can be concluded that the pressure ratio of 5.3 is a transition point. When the pressure ratio is higher than 5.3, the flow characteristics about mass flow rate and pressure distribution will change. Table 1 describes some parameters corresponding to the pressure-ratio transition point.

Table 1 Some parameters corresponding to the pressure-ratio transition point

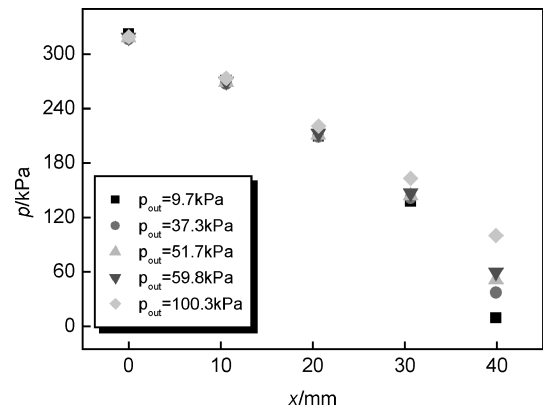
Inlet pressure, kPa	Outlet Mach number	Outlet Knudsen number	Pressure ratio	Reynolds number
130	0.0062	0.038	5.29	1.304
250	0.011	0.02	5.33	0.815
320	0.0139	0.0158	5.33	0.239



a) Inlet pressure of 130 kPa



b) Inlet pressure of 250 kPa



c) Inlet pressure of 320 kPa

Fig. 4 Pressure distributions for different inlet pressures.

From Table 1, it can be seen that when the pressure ratio is at the transition point the corresponding outlet Mach number and outlet Reynolds number are fairly small, but the outlet Knudsen number is relatively large. This is different from a macrochannel, which is considered to be a continuum flow, where the Knudsen number is much smaller. When a macrochannel flow reaches choking status, the outlet Reynolds number is much larger, and the outlet Mach number is close to unity.

III. Approximate Theoretical Analysis and Subchoking

Based on the experimental results, it can be found that when the inlet pressure is kept constant and pressure ratio is higher than approximately 5.3, mass flow rate changes little with the increase of pressure ratio. This phenomenon is analyzed by the approximate theoretical model.⁵ It is written as follows:

$$\dot{M} = \frac{wH^3 p_{in}^2}{24\mu RTL} \left[\left(1 - \frac{1}{\Pi_i^2}\right) + 12 \frac{2 - \sigma_v}{\sigma_v} \frac{Kn_{out} p_{out}}{p_{in}} \left(1 - \frac{1}{\Pi_i}\right) \right] \quad (1)$$

where

$$Kn_{out} p_{out} = \frac{\mu}{H} \sqrt{\frac{\pi RT}{2}}, \quad \sigma_v = 1$$

Equation (1) is applicable for $Kn \leq 0.1$. It can be seen that mass flow rate increases with the decrease of outlet pressure when keeping the inlet pressure constant. On the other hand, Tison's⁶ experimental

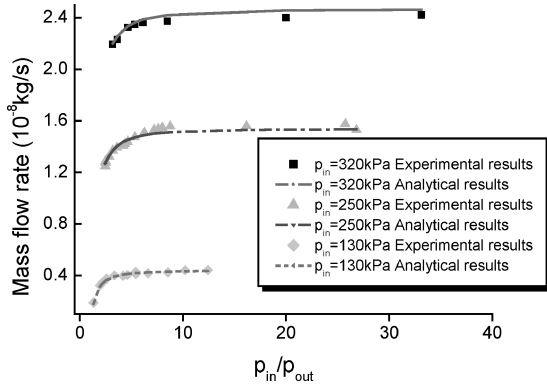
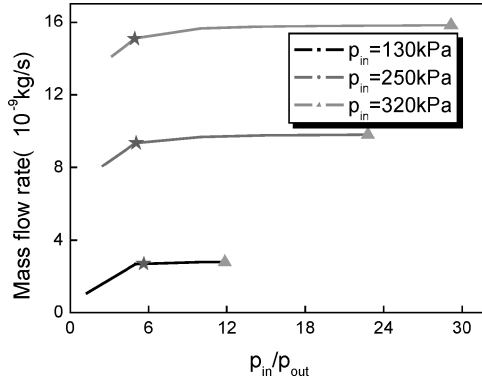
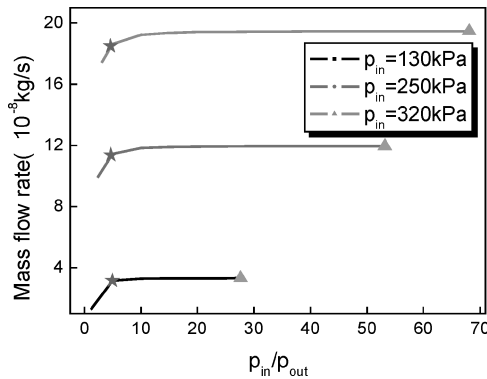


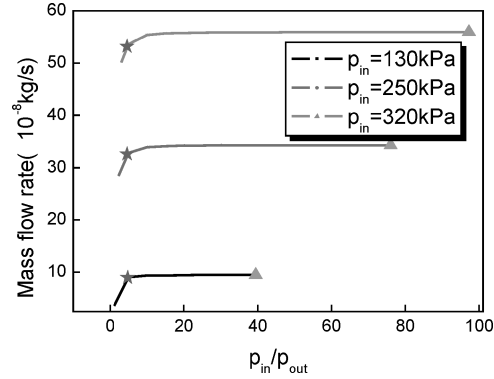
Fig. 5 Comparison of experimental data with analytical results.



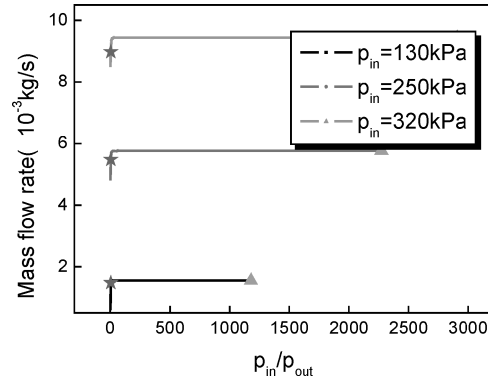
a) $S/V = 3.35 \times 10^5 \text{ m}^{-1}$



b) $S/V = 1.45 \times 10^5 \text{ m}^{-1}$



c) $S/V = 1.02 \times 10^5 \text{ m}^{-1}$



d) $S/V = 5.33 \times 10^3 \text{ m}^{-1}$

Fig. 6 Relationship between mass flow rate and pressure ratio.

results show that for transition flow or free molecule flow region, namely, $Kn > 0.1$, mass flow rate decreases with the increase of inlet-to-outlet pressure difference. As a result, it can be concluded that for the flow with $Kn \leq 0.1$, when Knudsen number is equal to 0.1, mass flow rate is up to maximum. So we introduce the following definitions:

1) When Knudsen number is equal to 0.1, mass flow rate reaches the maximum, namely, $(\dot{M})_{\max}$.

2) When the ratio of $|[\dot{M} - (\dot{M})_{\max}]/(\dot{M})_{\max}|$ is lower than 5%, the corresponding flow is defined as subchoking.

3) When the mass flow rate is up to 95% $(\dot{M})_{\max}$, the corresponding inlet-to-outlet pressure ratio is defined as subchoking critical pressure ratio.

Experimentally determined values of inlet-to-outlet pressure ratio vs mass flow rate are compared with the analytical results predicted by Eq. (1). Such a comparison is presented in Fig. 5. The excellent agreement can be seen.

The subchoking phenomenon is attributed to the surface effects in microchannel. The surface-to-volume ratio (S/V) in microchannel

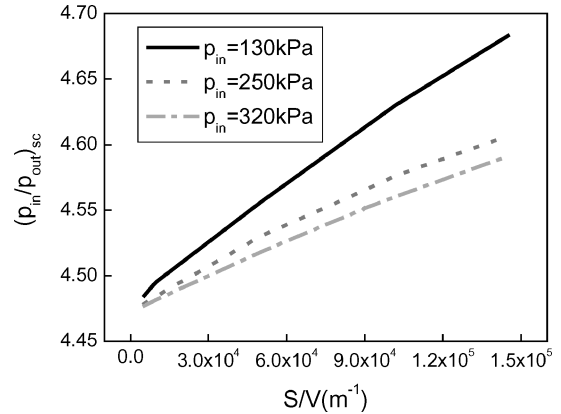


Fig. 7 Relationship between subchoking critical pressure ratio $(p_{in}/p_{out})_{sc}$ and the value of S/V .

is significantly higher than that in macrochannel. The relationship between the subchoking critical pressure ratio and the value of S/V is studied from the expression shown in Eq. (1). The results are shown in Fig. 6, where the asterisk shows that mass flow rate is equal to 95% $(\dot{M})_{\max}$, the corresponding x coordinate is subchoking critical pressure ratio $(p_{\text{in}}/p_{\text{out}})_{\text{sc}}$; the triangle shows that mass flow rate is equal to $(\dot{M})_{\max}$, and the corresponding x coordinate is the maximum of pressure ratio $(p_{\text{in}}/p_{\text{out}})_{\max}$.

From Fig. 6, it can be concluded that subchoking critical pressure ratio $(p_{\text{in}}/p_{\text{out}})_{\text{sc}}$ increases with the increase of the value of S/V .

Summarizing the results shown in Fig. 6, the curve of subchoking critical pressure ratio vs the value of S/V is described in Fig. 7. It clearly shows that subchoking critical pressure ratio of gas flow in microchannel $(p_{\text{in}}/p_{\text{out}})_{\text{sc}}$ increases with the increase of the value of S/V .

IV. Conclusions

Based on the microfabrication technology, a rectangular cross-section microchannel with distributed calibrating pressure points was fabricated. The flow characteristics of air were measured experimentally. During the experiment, the outlet pressure was lower than 1 atm. The relationship between outlet volume flow rate and inlet-to-outlet pressure ratio, pressure distribution, and inlet/outlet temperature were measured by regulating inlet or outlet pressure. The outlet pressure was lower than 1 atm, so that it was easy to realize multiregime mixedflow in a microchannel. Results indicate that keeping the inlet pressure constant at 130, 250, or 320 kPa

and decreasing the outlet pressure, when pressure ratio is approximately lower than 5.3, the mass flow rate increases with the increase of the pressure ratio; when pressure ratio is higher than 5.3, the mass flow rate changes little with the increase of pressure ratio. The phenomenon is defined as subchoking in this paper. The inlet-to-outlet pressure ratio corresponding to subchoking is defined as subchoking critical pressure ratio. The effect of the value of surface-to-volume ratio (S/V) on the subchoking critical pressure ratio is studied. Results indicate that with the increase of the value of (S/V), subchoking critical pressure ratio in microchannel increases.

Appendix A: Experimental Error Analysis

Based on the instruments and methods employed in our experiments, the uncertainties of our basic measured parameters are evaluated as follows:

- 1) The dimensions of the microchannels were measured by a calibrated scanning electron microscope (Model CSM-950) with a resolution of 1%.
- 2) The pressures were measured by a high-precision pressure transducer (Model No. ZOC17, Scanivalve Corp.) with a resolution of 0.08% of full scale.
- 3) The flow rates were measured by a flowmeter (Model RK-1450) with a resolution of 1%.
- 4) The temperatures were measured by a thermocouple; the output signals were measured by a potentiometer (Model WR9000) with a resolution of 0.8%.

Appendix B: Experimental Data

Table B1 Inlet pressure of 130 kPa

No.	Inlet, kPa	Temperature, C	Point2, kPa	Point3, kPa	Point4, kPa	Outlet, kPa	Mass flow ($\times 10^{-8}$ kg/s)
1	133.2098	23.23	112.1953	89.0449	59.4868	10.7056	0.4428
2	130.7983	22.24	108.957	85.8755	58.7289	15.3219	0.4247
3	130.5227	22.34	109.646	86.22	57.6265	19.8004	0.4179
4	130.2471	22.41	109.7838	86.7712	58.0399	23.9344	0.4108
5	133.2787	22.99	112.4709	88.976	59.5557	24.5545	0.4285
6	133.2098	22.44	117.4317	100	80.9836	60.0993	0.3496

Table B2 Inlet pressure of 250 kPa

No.	Inlet, kPa	Temperature, C	Point2, kPa	Point3, kPa	Point4, kPa	Outlet, kPa	Mass flow ($\times 10^{-8}$ kg/s)
1	250.4776	21.84	210.5156	162.9746	107.3034	9.3276	1.529
2	253.2336	19.73	212.5137	164.766	109.9216	31.5823	1.546
3	251.5111	19.98	212.5137	167.2464	112.7465	40.1259	1.507
4	250.3398	20.35	213.8936	170.3842	119.6068	46.947	1.4754
5	251.3733	23.46	218.0257	179.9929	139.4797	100.2756	1.276

Table B3 Inlet pressure of 320 kPa

No.	Inlet, kPa	Temperature, C	Point2, kPa	Point3, kPa	Point4, kPa	Outlet, kPa	Mass flow ($\times 10^{-8}$ kg/s)
1	322.6848	23.21	271.1476	209.8266	138.1017	9.741	2.5047
2	316.5527	23.33	267.2892	208.9998	141.34	37.301	2.3733
3	317.9996	23.46	269.0806	210.9979	144.096	51.7011	2.3605
4	318.6886	23.50	270.2519	212.7893	147.1276	59.7624	2.3475
5	319.102	23.56	273.5591	220.8506	163.1813	100.2756	2.1918

Acknowledgment

The research is supported by the National Science Foundation of China (No. 10272066).

References

- ¹Arkilic, E. B., Schmidt, M. A., and Breuer, K. S., "Gaseous Slip Flow in Long Microchannels," *Journal of Microelectromechanical Systems*, Vol. 6, No. 2, 1997, pp. 167–178.
- ²Liu, J. Q., Tai, Y. C., and Ho, C. M., "MEMS for Pressure Distribution Studies of Gaseous Flows in Microchannels," *Proceedings of the IEEE Micro Electro Mechanical Systems (MEMS)*, Inst. of Electrical and Electronics Engineers, Piscataway, NJ, 1995, pp. 209–215.
- ³Shih, J. C., Ho, C. M., and Liu, J. Q., "Monoatomic and Polyatomic Gas Flow Through Uniform Microchannels," *American Society of Mechanical Engineers, Dynamic Systems and Control Division (DSC)*, v 59, *Micro-Electro-Mechanical Systems (MEMS)*, American Society of Mechanical

Engineers, New York, 1996, pp. 197–203.

⁴Pong, K., Ho, C., and Liu, J., "Non-Linear Pressure Distribution in Uniform Microchannels," *American Society of Mechanical Engineers, Fluids Engineering Division (FED)*, v 197, *Application of Microfabrication to Fluid Mechanics*, American Society of Mechanical Engineers, New York, 1994, pp. 51–56.

⁵Arkilic, E. B., Breuer, K. S., and Schmidt, M. A., "Gaseous Flow in Microchannels," *American Society of Mechanical Engineers, Fluids Engineering Division (FED)*, v 197, *Application of Microfabrication to Fluid Dynamics*, American Society of Mechanical Engineers, New York, 1994, pp. 57–65.

⁶Tison, S., "Experimental Data and Theoretical Modeling of Gas Flows Through Metal Capillary Leaks," *Vacuum*, Vol. 44, 1993, pp. 1171–1175.

C. Kaplan
Associate Editor

J A C I C

Journal of Aerospace Computing, Information, and Communication

Editor-in-Chief: Lyle N. Long, Pennsylvania State University

AIAA has launched a new professional journal, the *Journal of Aerospace Computing, Information, and Communication*, to help you keep pace with the remarkable rate of change taking place in aerospace. And it's available in an Internet-based format as timely and interactive as the developments it addresses.

Scope:

This journal is devoted to the applied science and engineering of aerospace computing, information, and communication. Original archival research papers are sought which include significant scientific and technical knowledge and concepts. The journal publishes qualified papers in areas such as real-time systems, computational techniques, embedded systems, communication systems, networking, software engineering, software reliability, systems engineering, signal processing, data fusion, computer architecture, high-performance computing systems and software, expert systems, sensor systems, intelligent sys-

tems, and human-computer interfaces. Articles are sought which demonstrate the application of recent research in computing, information, and communications technology to a wide range of practical aerospace engineering problems.

Individuals: \$40 • Institutions: \$380

➔ **To find out more about publishing in or subscribing to this exciting new journal, visit www.aiaa.org/jacic, or e-mail JACIC@aiaa.org.**



American Institute of Aeronautics and Astronautics